AN INVESTIGATION OF ANISOTROPY OF OF 3D PERIODIC CELLULAR STRUCTURE DESIGS

Li Yang
Department of Industrial Engineering, University of Louisville, Louisville, KY 40292

Abstract

In the design of periodic cellular structures, there exist various isotropic unit cell designs that possess identical theoretical mechanical properties along three or multiple principal symmetry directions. Although such definition of "isotropy" differs from the traditional definition that is used for solid materials, it is often considered to represent the equivalent design implications in many applications. In this study, the mechanical properties of various 2D and 3D periodic cellular structures under uniaxial stress along different non-principal directions were investigated. The relationships between the cellular unit cell geometries, structural size, loading orientation and the mechanical properties of the cellular structures made of perfect elastic-plastic material were discussed, which provide insights into the future design of cellular structures when utilizing homogenization treatments.

Keywords: v

Introduction

Cellular structures are often treated as metamaterials that exhibit mechanical and physical properties that can be tailored at broad ranges by both the geometry and material designs [1-6]. Traditional design theories for cellular structures focus on the design of relatively few parameters such as the relative densities and the characterization of the relationships between the pore characteristics and the structural properties [1, 2, 7-9], which is partly due to the lack of geometry control of the cellular structures with the traditional manufacturing processes [10, 11]. With the rapid emergence of additive manufacturing (AM), manufacturability no longer poses insurmountable challenges for the cellular structures, which allows for more sophisticated design methods to be applied to the cellular designs for more optimized performance [6, 12-14]. One of the common methods for the modeling of the cellular structures is the homogenization method, which treats the cellular structures as continuum with equivalent material properties [15-17]. The equivalent material properties for the cellular structures can be established through either analytical modeling, experimentation or numerical analysis, including the elastic modulus, the shear modulus and the Poisson's ratios of the structures, which allows for the development of the constitutive material properties for the equivalent materials. It has been shown that the cellular structure-equivalent materials exhibit rather unique yield surfaces under multi-axial loadings that are not seen with regular solid materials [18, 19], which implies that the transformation law generally applied to continuum must be subjected to more scrutiny. In general materials exhibit either isotropic properties or specific anisotropic properties (e.g. transversely isotropic, orthotropic), and in various literatures the homogenized cellular structures are treated as orthotropic materials [20-23], which have the general constitutive elastic properties in the form of Eq.(1):

$$\begin{bmatrix} \varepsilon_{11} \\ \varepsilon_{22} \\ \varepsilon_{33} \\ 2\varepsilon_{23} \\ 2\varepsilon_{31} \\ 2\varepsilon_{12} \end{bmatrix} = \begin{bmatrix} \frac{1}{E_{11}} & -\frac{\nu_{23}}{E_{22}} & -\frac{\nu_{31}}{E_{33}} & 0 & 0 & 0 \\ -\frac{\nu_{12}}{E_{11}} & \frac{1}{E_{22}} & -\frac{\nu_{32}}{E_{33}} & 0 & 0 & 0 \\ -\frac{\nu_{13}}{E_{11}} & -\frac{\nu_{23}}{E_{22}} & \frac{1}{E_{33}} & 0 & 0 & 0 \\ 0 & 0 & 0 & \frac{1}{G_{23}} & 0 & 0 \\ 0 & 0 & 0 & 0 & \frac{1}{G_{31}} & 0 \\ 0 & 0 & 0 & 0 & 0 & \frac{1}{G_{12}} \end{bmatrix} \begin{bmatrix} \sigma_{11} \\ \sigma_{22} \\ \sigma_{33} \\ \sigma_{23} \\ \sigma_{31} \\ \sigma_{12} \end{bmatrix} \quad \text{or } \varepsilon = C\sigma \quad (1)$$

For the material modeling with continuum, the concepts for transformation law and principal stress are well understood. However, for cellular structures the continuity assumption does not hold valid at dimensional scale comparable to the unit cell dimensions. Therefore, the concept of orthotropy and isotropy must be subjected to extra care. For examples, for the unit cell designs shown in Fig.1, although they are sometimes considered as “isotropic” designs, it can be seen that these designs essentially exhibit identical geometrical topologies only along specific directions that are governed by structural symmetry. There is no guarantee that the structures would exhibit the same mechanical properties along the directions that are not aligned with these symmetrical axles. The lack of structural symmetries along these directions not only introduces significant potential property variabilities but also renders the homogenization approach questionable.

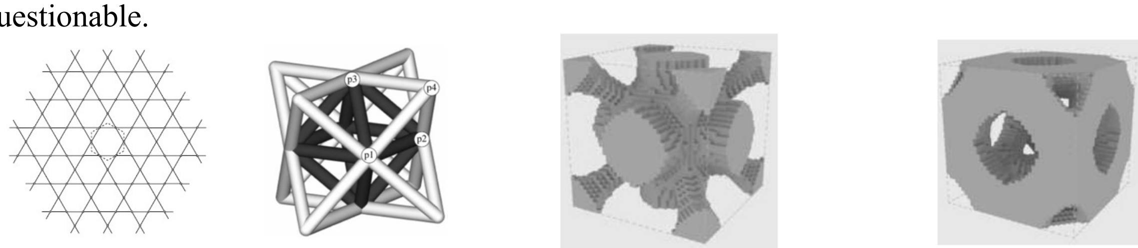

a. 2D Kagome [24] b. Octet-truss [19] c. Optimized schwartz 1 [25] d. Optimized schwartz 2 [25]

Fig.1 Examples of “isotropic” unit cell designs

However, designing cellular structures with unit cells not aligned along their symmetrical directions can be challenging largely due to the difficulty of treatment with the boundaries. With these alignments, the boundaries of a regular design space would likely include incomplete unit cells as illustrated in Fig.2. These incomplete unit cells could potentially contribute to the structural strength but are inherently difficult to model using analytical methods. On the other hand, the use of finite element analysis can be time consuming. For large cellular structures with sufficient number of unit cells, such boundary effects might be negligible. However, for relatively small cellular structures, such issue might become prominent. As there is a general lack of knowledge with this subject, in this paper we attempted to use simulation based study to identify the significance of this anisotropy issue with cellular structures loaded along varying directions.

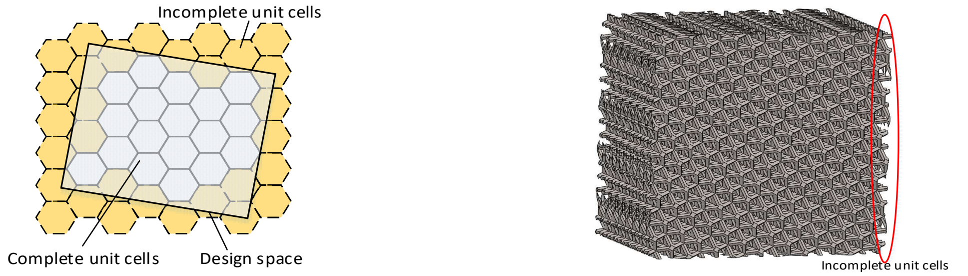

a. 2D honeycomb b. 3D BCC lattice

Fig.2 Examples of incomplete unit cells on boundaries due to pattern misalignment

Experiments

Three types of unit cells were used for this study, which are the re-entrant auxetic, the octet-truss, and the BCC structures. The geometrical design parameters of each type of unit cell are shown in Fig.3. These unit cell structures are expected to represent different cellular mechanisms. The re-entrant auxetic structure exhibits negative Poisson's ratios, and is a bending-dominated structure that exhibits directionally anisotropic mechanical properties (i.e. different mechanical properties along different principal directions). From previous studies it was also known that the re-entrant auxetic structure exhibits minimum cellular size effects, which means that the number of unit cells along each of the principal directions (i.e. x, y or z directions shown in Fig.3a) does not affect the mechanical properties of the structures [26]. The octet-truss structure is a stretch-dominated structure that exhibits directionally isotropic mechanical properties. The mechanical properties of the octet-truss structures have been extensively modeled [11, 19, 20]. It was shown that the octet-truss structures exhibit significant size effects that are also dependent on the unit cell number aspect ratios along different principal directions. The BCC structure is a bending-dominated structure that could exhibit either directionally isotropic or anisotropic behaviors depending on the geometry designs. In addition, the BCC structure also exhibit significant size effects that are also dependent on the aspect ratios of unit cell numbers in different directions [27]. The geometry designs of the unit cells in this study are listed in Table 1. For each cellular designs, cellular patterns were created and loaded along various directions for the anisotropy study. The size effects of these cellular designs were evaluated previously, which provided additional reference information for the current study [26].

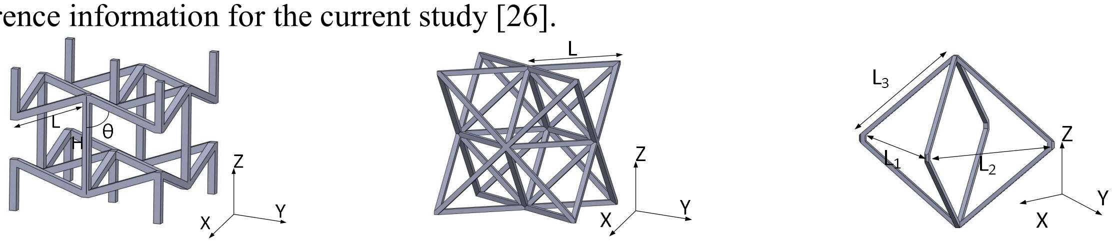

a. Re-entrant auxetic b. Octet-truss c. BCC

Fig.3 Unit cell designs

Design	H (L_1)	L (L_2)	θ (L_3)	Relative density
Auxetic 1 (Aux1)	4.2mm	3.6mm	70°	0.16-0.17
Auxetic 2 (Aux2)	7mm	3.5mm	50°	0.16-0.18
Octet-truss 1 (Oct1)		5mm		0.18-0.19
BCC-1	3.3mm	6.6mm	4.46mm	0.16-0.17

BCC-2	4.6mm	4.6mm	3.98mm	0.16-0.17

Table 1 Geometry designs of unit cells

Fig.4 shows the design of the cellular structures for uniaxial compressive loadings. The overall cellular structures were designed to have cuboid envelopes, and were sandwiched between two stiff platens (1000x elastic modulus) for compressive loading. For all the designs, the structures were only rotated by the x-axis, therefore only the anisotropy in the y-z planes was investigated. Structures with rotational angles of 15°, 30°, 45°, 60° and 75° were created. Due to the misalignment issue, it is difficult to achieve accurate number of unit cell control. Therefore, the dimension design for the structure followed the estimation method shown in Fig.4c, which uses the smaller dimension of the diagonal bounding box (d_1 and d_2) of the rotated unit cells as the reference dimensions. For most structures, the in-plane dimensions (D_1 and D_2) were designed to vary from approximately 3x, 7x and >10x of the reference dimensions. Due to the performance limitation of the computers used for this study, with some design variations the largest achievable dimensions for the cellular structures are less than 10x the reference dimensions, and the smaller dimensions of that design had to be adjusted accordingly. For all the designs the thickness (D_3) of the structures were fixed at 8x unit cell thickness. Some of the designs are shown in Fig.5 as examples of design permutations with both overall dimensions and orientation angles.

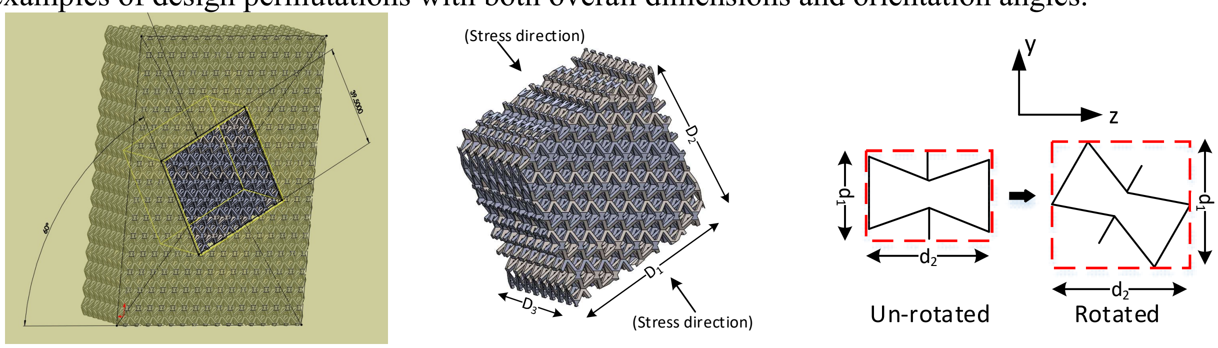

a. Design scheme b. Overall dimensions c. Reference unit dimension

Fig.4 Design of the cellular structures

All the modeling and simulations were performed using SolidWorks. Ti6Al4V was used as the material for simulations although such selection is largely arbitrary. Uniaxial compressive loading of 0.1MPa was applied in all instances. The displacement of the cellular structures were obtained after the simulations and used to calculate the normal and shear strains resulted from the normal stresses. In addition, the elastic modulus of the structures were also calculated. Fig.6 illustrate the finite element analysis (FEA) of the re-entrant auxetic structure Aux1 with 75° orientation angle.

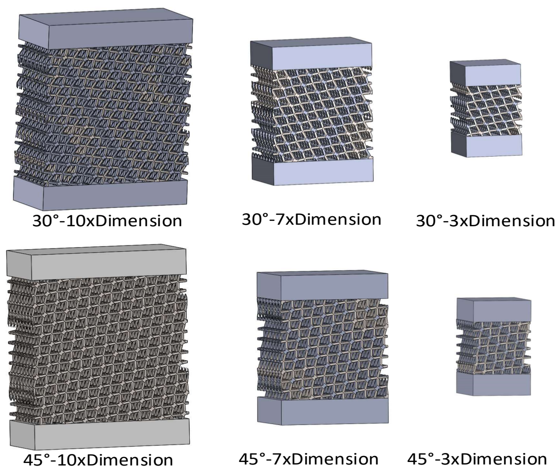

Fig.5 Some cellular structures with BCC1 unit cell design

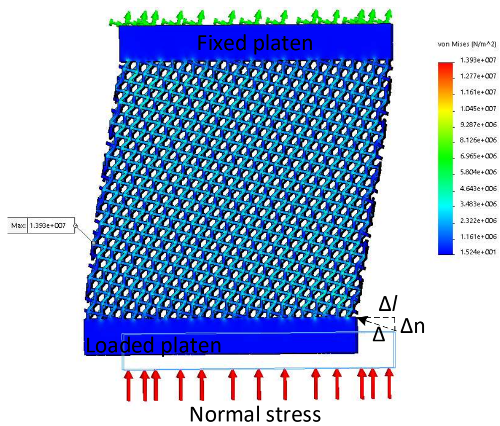

Fig.6 FEA analysis of the cellular structures

<u>Results and Discussions</u>

Fig.7 shows the rotational angle-elastic modulus relations for the two auxetic designs at varying overall dimensions. Using the previously introduced method for the cellular design size estimations, it is shown that the auxetic structures also exhibit minimum size effects upon rotation. It was previously shown that the re-entrant auxetic structures exhibit stabilized size effects when the numbers of unit cells are larger than 2, which was also the case in the current study [26]. On the other hand, the elastic modulus of the cellular structures exhibit directional differences. Fig.8 further illustrates such rotational angle dependency using the largest auxetic cellular structures of each rotational angle as examples. The re-entrant auxetic structures exhibit lowest elastic modulus between the rotational angles of 30°-60°. The consistency of the trend between the two auxetic designs is somewhat unexpected, as it was assumed that the geometrical design parameters would have certain effects on the anisotropic behaviors. Also, compared with the non-rotated structures, the Aux2 exhibits significant weakening, which is possibly due to the loss of compression mode of the vertical struts that have more significant contributions to elastic modulus in Aux2 designs [28]. Also, it was noticed that the Aux1 structure rotated by 75° exhibits higher elastic modulus compared to the non-rotated baseline, which might be contributed by the alignment of some of the re-entrant struts along the loading direction as shown in Fig.9.

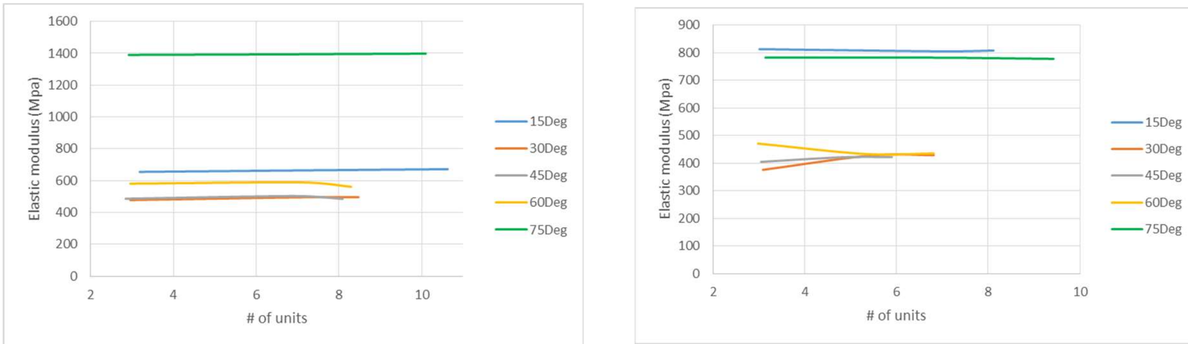

a. Aux1 b. Aux2

Fig.7 Rotational angle-elastic modulus relationships for auxetic structures with varying dimensions

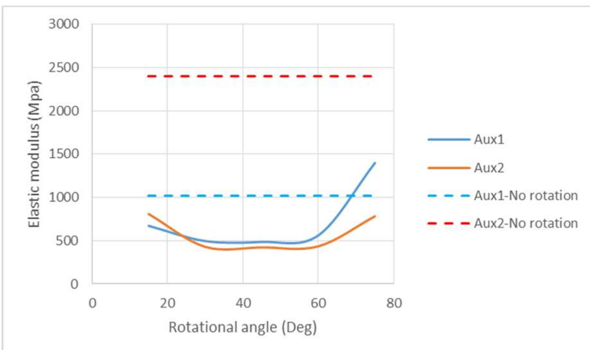

Fig.8 Rotataional angle-elastic modulus of auxetic structures

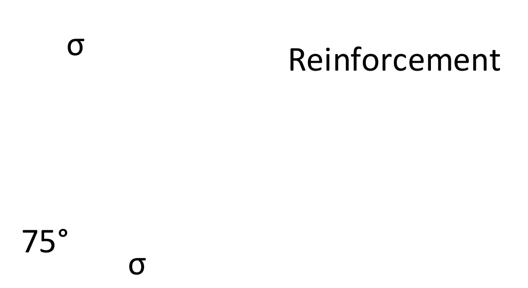

Fig.9 Reinforcement effect due to rotation

A perhaps equally interesting observation with the simulation results is the occurrence of significant stress concentration effects for rotated auxetic structures. As shown in Fig.10, when the re-entrant auxetic structures rotated between 30°-60° are compressed, they exhibit stress concentration patterns that spread along the diagonal lines of the overall cellular structures. Such stress concentration pattern was observed previously only with BCC structures when loaded along the principal direction [27]. Additional investigations are underway to further identify this phenomenon.

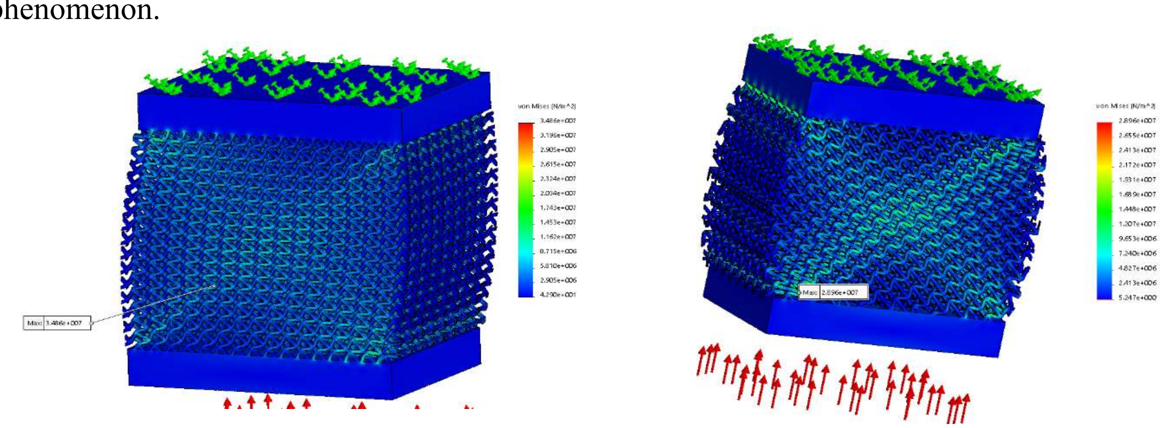

a. Aux1 b. Aux2

Fig.10 Von Mises stress of auxetic structures rotated by 45°

Fig.11 shows the rotational angle-elastic modulus relationships of the two BCC structures at varying overall dimensions. BCC1 exhibits directionally anisotropic design, and it can be seen that the rotated structures exhibit size effects that stabilizes at number of unit cells >4. BCC2 exhibits more directionally isotropic design, and the size effects for the rotated BCC2 appear more significant without obvious stabilizing levels. Fig.12 illustrates the change of elastic modulus for BCC structures with certain structural dimension levels. For both BCC designs the maximum elastic modulus levels were achieved at rotational angles of around 45°-50°, again likely due to the realignment of the struts towards the loading directions. Since for the BCC structure the elastic modulus is directly related to the alignment angle between the struts and the loading direction, the rotation of the structure could potentially result in enhanced elastic modulus. Again size effect is apparent rom Fig.12b for BCC2. With increasing overall cellular dimensions the elastic modulus of the structures reduces, which agrees with the previous observation. The fact that the BCC1 exhibits diminished size effects implies that the size effects for cellular structure is not intrinsic to geometry designs, which should be further explored in the future.

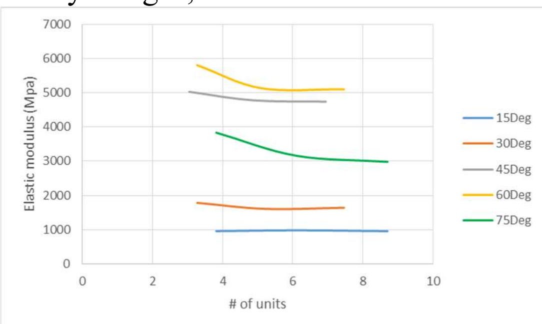

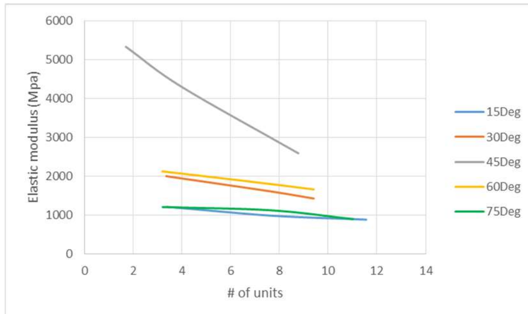

a. BCC1 b. BCC2

Fig.11 Rotational angle-elastic modulus relationships for BCC structures with varying dimensions

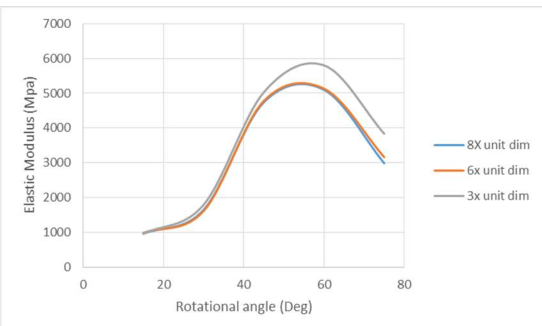

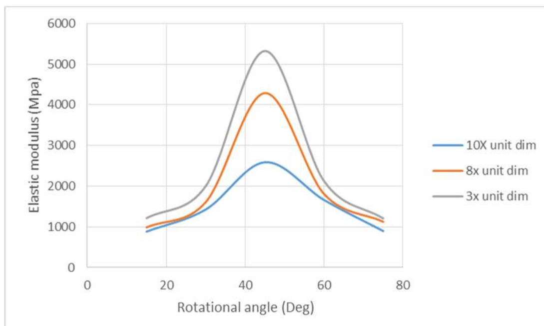

a. BCC1 b. BCC2

Fig.12 Rotataional angle-elastic modulus of BCC structures

Fig.13 shows the simulation results of stress distributions for the rotated BCC structures. It was observed that for all the rotated BCC structures the diagonal stress concentration patterns did not occur. From the perspective of cellular design this can possibly be considered as generally favorable, as more uniform and periodic stress distributions could potentially increase both the strength and the energy absorption efficiency of the structures.

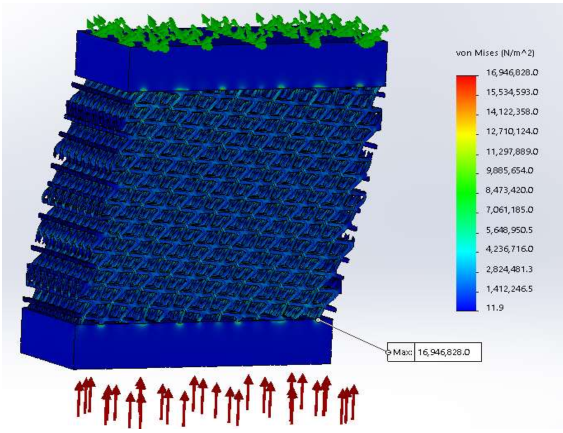

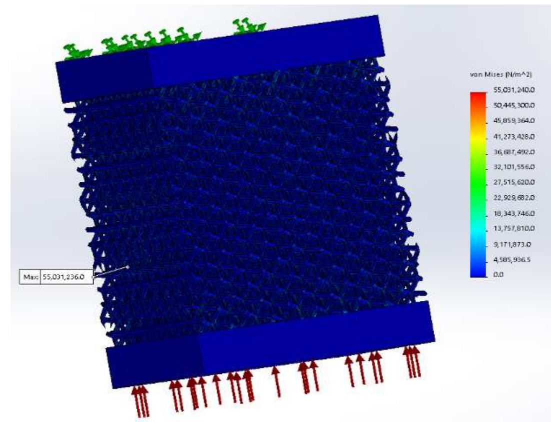

a. BCC1 b. BCC2

Fig.13 Von Mises stress of BCC structures rotated by 30°

The rotational angle-elastic modulus relationships for the octet-truss structures with varying overall dimensions are shown in Fig.14a. Due to the high level of symmetry with the octet-truss structures, simulations were only performed with 15°, 30° and 45°, as the structures with 60° and 75° rotational angle are essentially identical to structures with 30° and 15° rotational angles, respectively. The octet-truss structures exhibit very small size effects that stabilizes at >2 unit dimensions, and the relationship between the elastic modulus and the rotational angle also appears regular. On the other hand, despite the conventional notion that the octet-truss structure is isotropic, there exist ~25-30% difference of elastic properties between the rotated structures and the non-rotated structures. The rotation generally tend to enhance the elastic modulus, which can be attributed to the alignment of struts along the loading direction, as can be seen from Fig.14b clearly for 45°-rotation octet-truss. In this particular case since some of the struts become vertically aligned to the loading direction, the maximum enhancement effect is achieved.

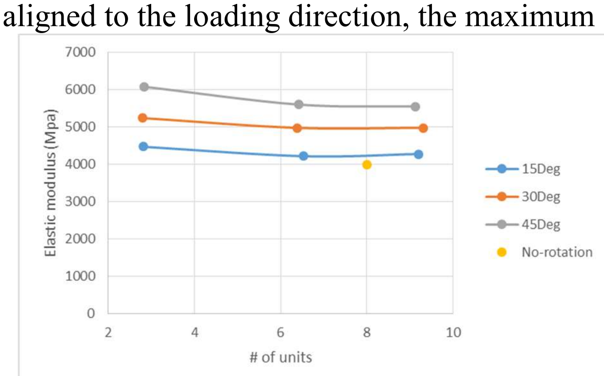

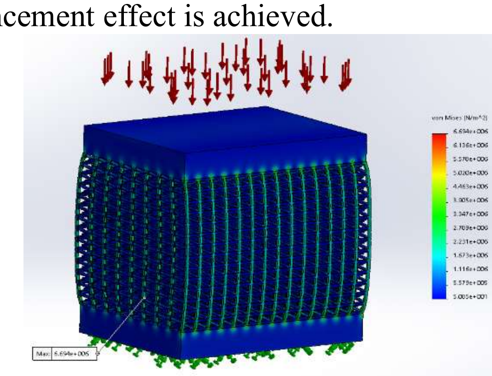

a. Rotational angle-elastic modulus relationships

b. Von Mises stress of octet truss structure rotated by 45°

Fig.14 Rotated octet-truss structures

Conclusions

In this paper simulation based studies were employed to investigate the elastic properties of three cellular structures (re-entrant auxetic, BCC, octet-truss) under various rotational angles. The re-entrant auxetic structures exhibit minimum size effects regardless of the geometry designs, which clearly indicates that the minimized size effect is an intrinsic attribute for this type of cellular geometry. The BCC structures still exhibit size effects, although the significance of the size effects for BCC structures with all rotational angles appears to be dependent on the geometry design parameter of the BCC, with more directionally isotropic designs exhibit more significant size effects similar to that observed previously with non-rotated BCC structures. The rotated octet-truss structure exhibit very small size effects that differ from the previous observations. All cellular designs exhibit anisotropic elastic properties, while the degree of anisotropy appears to be related to the specific geometrical parameters of the structures, especially in the case of BCC structures. Lastly, loading along different orientations appears to alter the stress concentration patterns significantly for all the structures investigated in this study. Further investigations is needed to fully identify such effects.

Acknowledgements

The author is grateful of the support of the Office of Naval Research Grant #N00014-16-1-2394 and helpful discussions with Dr. Richard Fonda.

Reference

[1] L. J. Gibson, M. F. Ashby. Cellular Solids: Structure and Properties. 2nd Edn. Cambridge University Press, 1997.

[2] M. F. Ashby, A. G. Evans, N. A. Fleck, L. J. Gibson, J. W. Hutchinson, H. N. G. Wadley. Metal Foams: A Design Guide. Butterworth Heinemann, 2000.

[3] T. J. Lu, H. A. Stone, M. F. Ashby. Heat transfer in open-cell metal foams. Acta Materialia. 46(1998), 10: 3619-3635.

[4] I. Schmidt, N. A. Fleck. Ductile fracture of two-dimensional cellular structures. International Journal of Fracture. 111(2001): 327-342.

[5] H. N. G. Wadley. Multifunctional periodic cellular metals. Philosophical Transactions of the Royal Society A. 364(2006): 31-68.

[6] C. C. Seepersad, B. M. Dempsey, J. K. Allen, F. Mistree, D. L. McDowell. Design of multifunctional honeycomb materials. AIAA Journal. 42(2004), 5: 1025-1033.

[7] E. Amsterdam, H. van Hoorn, J. th. M. De Hosson, P. R. Onck. The influence of cell shape anisotropy on the tensile behavior of open cell aluminum foam. Advanced Engineering Materials. 10(2008), 9: 877-891.

[8] W.-Y. Jang, S. Kyriakides. On the crushing of aluminum open-cell foams: part II analysis. International Journal of Solids and Structures. 46(2009): 635-650.

[9] A.-M. Harte, N. A. Fleck, M. F. Ashby. Fatigue failure of an open cell and a closed cell aluminum alloy foam. Acta Materialia. 47(1999), 8: 2511-2524.

[10] J. Banhart. Manufacture, characterisation and application of cellular metals and metal foams. Progress in Materials Science. 46(2001): 559-632.

[11] H. N. G. Wadley, N. A. Fleck, A. G. Evans. Fabrication and structural performance of periodic cellular metal sandwich structures. Composites Science and Technology. 63(2003): 2331-2343.

[12] C. B. Williams, J. K. Cochran, D. W. Rosen. Additive manufacturing of metallic cellular materials via three-dimensional printing. International Journal of Advanced Manufacturing Technologies. 53(2011): 231-239.

[13] P. Heinl, A. Rottmair, C. Korner, Robert F. Singer. Cellular titanium by selective electron beam melting. Advanced Engineering Materials. 9(2007), 5: 360-364.

[14] D. A. Ramirez, L. E. Murr, S. J. Li, Y. X. Tian, E. Martinez, J. L. Martinez, B. I. Machado, S. M. Gaytan, F. Medina, R. B. Wicker. Open-cellular copper structures fabricated by additive manufacturing using electron beam melting. Materials Science and Engineering A. 528(2011): 5379-5386.

[15] S. Arabnejad, D. Pasini. Mechanical properties of lattice materials via asymptotic homogenization and comparison with alternative homogenization methods. International Journal of Mechanical Sciences. 77(2013): 249-262.
[16] H. V. Wang, S. R. Johnston, D. W. Rosen. Design of a graded cellular structure for an acetabular hip replacement component. Proceedings of the International Solid Freeform Fabrication Symposium, Austin, TX, 2006.
[17] C. Florence, K. Sab. A rigorous homogenization method for the determination of the overall ultimate strength of periodic discrete media and an application to general hexagonal lattices of beams. European Journal of Mechanics A/Solids. 25(2006): 72-97.
[18] E. M. K. Abad, S. A. Khanoki, D. Pasini. Fatigue design of lattice materials via computational mechanics: application to lattices with smooth transitions in cell geometry. International Journal of Fatigue. 47(2013): 126-136.
[19] V. S. Deshpande, N. A. Fleck, M. F. Ashby. Effective properties of the octet-truss lattice material. Journal of the Mechanics and Physics of Solids. 49(2001): 1747-1769.
[20] L. Dong, V. Deshpande, H. Wadley. Mechanical response of Ti-6Al-4V octet-truss lattice structures. International Journal of Solids and Structures. 60-61(2015): 107-124.
[21] P. Zhang, J. Toman, Y. Yu, E. Biyikli, M. Kirca, M. Chmielus, A. C. To. Efficient design-optimization of variable-density hexagonal cellular structure by additive manufacturing: theory and validation. Journal of Manufacturing Science and Engineering. 137(2015): 021004.
[22] M. S. A. Elsayed, D. Pasni. Multiscale structural design of columns made of regular octet-truss lattice material. International Journal of Solids and Structures. 47(2010): 1764-1774.
[23] A. Vigliotti, D. Pasini. Mechanical properties of hierarchical lattices. Mechanics of Materials. 62(2013): 32-43.
[24] V. J. Challis, A. P. Roberts, A. H. Wilkins. Design of three dimensional isotropic microstructures for maximized stiffness and conductivity. International Journal of Solids and Structures. 45(2008), 14-15: 4130-4146.
[25] R. G. Hutchinson, N. A. Fleck. The structural performance of the periodic truss. Journal of the Mechanics and Physics of Solids. 54(2006): 756-782.
[26] L. Yang. A study about size effects of 3D periodic cellular structures. Proceedings of the International Solid Freeform Fabrication Symposium, Austin, TX, 2016.
[27] L. Yang. Experimental-assisted design development for an octahedral cellular structure using additive manufacturing. Rapid Prototyping Journal. 21(2015), 2: 168-176.
[28] L. Yang, O. Harrysson, H. West, D. Cormier. Mechanical properties of 3D re-entrant honeycomb auxetic structures realized via additive manufacturing. International Journal of Solids and Structures. 69-70(2015): 475-490.